The Journal of Supercritical Fluids 199 (2023) 105969

Contents lists available at ScienceDirect

The Journal of Supercritical Fluids

journal homepage: www.elsevier.com/locate/supflu

Sorbitol-coated indomethacin and naproxen particles produced by supercritical CO_2-assisted spray drying

Fidel Méndez Cañellas [a,b,c], Robert Geertman [c], Lidia Tajber [b,d], Luis Padrela [a,b,*]

[a] Department of Chemical Sciences, Bernal Institute, University of Limerick, Limerick V94 T9PX, Ireland
[b] SSPC, the SFI Research Centre for Pharmaceuticals, Bernal Institute, University of Limerick, Limerick V94 T9PX, Ireland
[c] Janssen Pharmaceutica NV, 2340 Beerse, Belgium
[d] School of Pharmacy and Pharmaceutical Sciences, Trinity College Dublin, College Green, D02 PN40 Dublin 2, Ireland

HIGHLIGHTS

- SASD yielded naproxen crystalline Form 1 particles in an amorphous sorbitol matrix.
- SASD yielded a partially crystalline indomethacin-sorbitol mixture.
- SASD produced naproxen and indomethacin particles in the range of 0.4–7.6 μm.
- The sorbitol matrix dissolved upon contact with water releasing naproxen particles.
- COSMO-RS modelling and DSC provided insights into the API-sorbitol system.

GRAPHICAL ABSTRACT

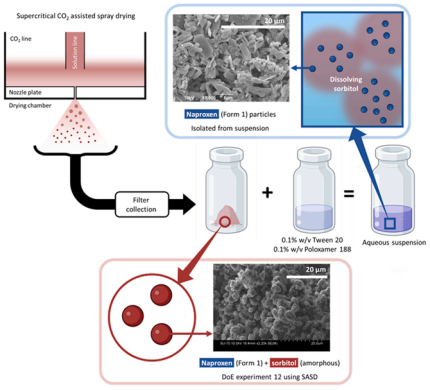

ARTICLE INFO

Keywords:
Active pharmaceutical ingredients
Polymorphism
Microparticles
Supercritical CO_2
Design of experiments

ABSTRACT

Co-spraying active pharmaceutical ingredients (APIs) with excipients is a strategy to create excipient matrices containing API particles to address formulation challenges such as the reconstitution of powders into homogeneous suspensions. In this work, indomethacin and naproxen were co-sprayed with/without sorbitol using supercritical CO_2-assisted spray drying (SASD), followed by particle collection in a filter paper, and resuspension in an aqueous excipient solution. SASD yielded particles in the range of 0.4–7.6 μm, naproxen crystalline Form 1 particles in an amorphous sorbitol matrix, and a partially crystalline indomethacin-sorbitol mixture. Most naproxen-sorbitol mixtures successfully constituted homogenous microparticle suspensions where sorbitol matrix dissolved upon contact with water releasing naproxen particles, while indomethacin-sorbitol mixtures were not reconstitutable and not studied further. The API-sorbitol interactions were studied in detail by thermal analysis and COSMO-RS modelling. Overall, the work presented herein provides a better understanding of co-spraying of APIs with excipients for the formulation of reconstitutable dried microparticles.

* Corresponding author at: Department of Chemical Sciences, Bernal Institute, University of Limerick, Limerick V94 T9PX, Ireland.
E-mail address: Luis.Padrela@ul.ie (L. Padrela).

https://doi.org/10.1016/j.supflu.2023.105969
Received 22 February 2023; Received in revised form 18 April 2023; Accepted 3 May 2023
Available online 5 May 2023

1. Introduction

Particle size reduction has become an increasingly popular strategy to enhance the dissolution rate of active pharmaceutical ingredients (APIs) with low aqueous solubility such as those falling into the Biopharmaceutics Classification System (BCS) class II. According to the Noyes Whitney equation, smaller particles have a higher surface-to-volume ratio which implies an enhanced contact with water molecules, and thus, an enhanced dissolution rate [1–3]. Nano- and microparticles are commonly formulated as crystalline particles in aqueous media containing stabilizers/excipients for parenteral administration [2,4–8]. In this case, the dissolution rate upon parenteral administration depends on the surface area of the crystals and the dissolution kinetics at the targeted tissue fluid [7,8]. Accurate control over the API solid form and particle size in aqueous suspensions is of paramount importance to ensure the desired drug release and efficacy during administration. This strategy can contribute to enhanced treatment of various diseases, for instance through their formulation as long-acting injectables (LAIs). Long-acting formulations typically release a drug for long periods (e.g. weeks to months) replacing the need for daily medication and thus improving patient adherence, convenience, and compliance [7,8].

The pharmaceutical industry follows two approaches to manufacture parenteral aqueous particle suspensions: ready-to-use (RTU) suspensions and powders for injection (also known as lyophilised powders for injection, two-vial approach or reconstituted mixtures). RTU suspensions have been successful in the delivery of small-volume parenteral formulations as these are contained in a closed system without the need for further manipulation [9]. Among parenteral commercial approaches, RTU suspensions are easier to administer, prevent risks related to the handling (e.g. preparation or calculation errors), and require less time for preparation [9]. Conversely, powders for injection need to be reconstituted into a suspension that can be injected [10]. For the latter approach, during the reconstitution and dilution process, it is key to achieve the right dose and stability of the parenteral formulation [10]. Reconstituted mixtures need to be handled by a medical professional to ensure sterility and dose accuracy, and thus, the process is prone to human errors [9–13]. However, powders for injection ensure that patients receive the accurate dose of medication as prescribed, giving greater flexibility in terms of dosing and administration and making it easier to customize the treatment for individual patients. Another key advantage of the latter approach is better long-term stability in comparison to RTU suspensions. Thus, a larger number of APIs can be formulated as powders for injection, due to the extended shelf stability, and solvents or excipients required for long-term stability, which might cause side effects, can be avoided. Overall, powders for injections offer several advantages over other forms of pharmaceuticals and are a good choice for drugs that require dosing flexibility and improved stability.

Typical methods to produce crystalline nano- and microparticles for the preparation of parenteral aqueous suspensions can be divided into top-down and bottom-up approaches. Bottom-up techniques build up particles from the molecular level where the control over particle properties such as the particle size distribution, morphology, and solid form is generally more feasible compared to top-down methods [14,15]. Conventional bottom-up techniques (e.g. liquid antisolvent precipitation, solvent evaporation) for the production of API particles require the use of organic solvents and extra steps to remove them from the final dry product. Conversely, techniques based on supercritical CO_2 can remove the organic solvent during processing and thus, overcome this limitation and also provide accurate control over the physicochemical properties of API particles in the micro- and nanometric range [16–20]. The dry product free of organic solvents can be obtained with supercritical CO_2 technology. Supercritical CO_2 can be used in various techniques to produce drug particles by acting as a solvent, antisolvent, on additive [19,21]. The main function of the supercritical CO_2 in the technique used in this work, namely supercritical CO_2-assisted spray drying (SASD), is to enhance the atomisation step. The desired particle size and solid form can be achieved with SASD by adjusting distinct processing parameters, such as the composition and ratio of the components of the sprayed solution (e.g. organic solvent, active pharmaceutical ingredient (API), excipient), the API solution and CO_2 flow rates, pressure, temperature (drying chamber and nozzle), and nozzle parameters (e.g. number of orifices, orifice diameter) [16–19,21,22]. The API model systems used in this work are indomethacin and naproxen, which belong to the BCS class II. There have been papers reported in the literature addressing particle production of these APIs using CO_2-based atomisation techniques [23–26]. For instance, naproxen crystalline particles with a median particle diameter of 10 μm were produced using depressurization of an expanded liquid organic solution (DELOS) [23]. Regarding indomethacin, cocrystals of this API with saccharin have been reported in the literature using supercritical fluid enhanced atomisation (SEA), and in combination with excipients that act as carriers such as PLGA and chitosan with supercritical assisted injection in a liquid antisolvent (SAILA) and supercritical assisted atomisation (SAA), respectively [24–26]. Moreover, microparticles of indomethacin presenting the α polymorph have been produced by Rodrigues et al. using the SEA method [27]. To the best of our knowledge, neither of these APIs has been processed using the SASD method, particularly to generate a reconstitutable powered formulation.

In this work, indomethacin and naproxen were sprayed using SASD with and without sorbitol followed by their collection in a filter. The hypothesis is that co-spraying each API with a water-soluble excipient (sorbitol) would facilitate the reconstitution of the spray-dried powder

Table 1
Experimental conditions used in CO_2-assisted spray drying runs for a Design of Experiments (DoE) using naproxen and indomethacin as API model systems.

DoE experimental run	Solvent	Co-sprayed excipient	*P* (MPa)	F_{liquid} (mL/min)	F_{liquid} (g/min)[a]	F_{CO2} (g/min)	$R_{liquid/CO2} \times 100$
1	Methanol	No excipient	10	0.1	0.081	25	0.324
2			15	0.1	0.081	40	0.203
3			15	0.4	0.324	40	0.810
4			10	0.4	0.324	25	1.296
5	Acetone		10	0.1	0.081	25	0.324
6			15	0.1	0.081	40	0.203
7			15	0.4	0.324	40	0.810
8			10	0.4	0.324	25	1.296
9	Methanol	Sorbitol	10	0.1	0.083	25	0.332
10			15	0.1	0.083	40	0.208
11			15	0.4	0.332	40	0.830
12			10	0.4	0.332	25	1.328

P: pressure inside the high-pressure nozzle. F_{liquid}: mass solution flow rate. F_{CO2}: mass supercritical CO_2 flow rate. $R_{liquid/CO2}$: mass flow-rate ratio of the solvent to supercritical CO_2. For all CO_2-assisted spray drying experiments, the sprayed volume was 20 mL, temperature in the nozzle and drying chamber was 50 °C, concentration of API and Sorbitol was 20 mg/mL each.
[a] Densities used for acetone and methanol were 0.790 g/mL and 0.791 g/mL, respectively.

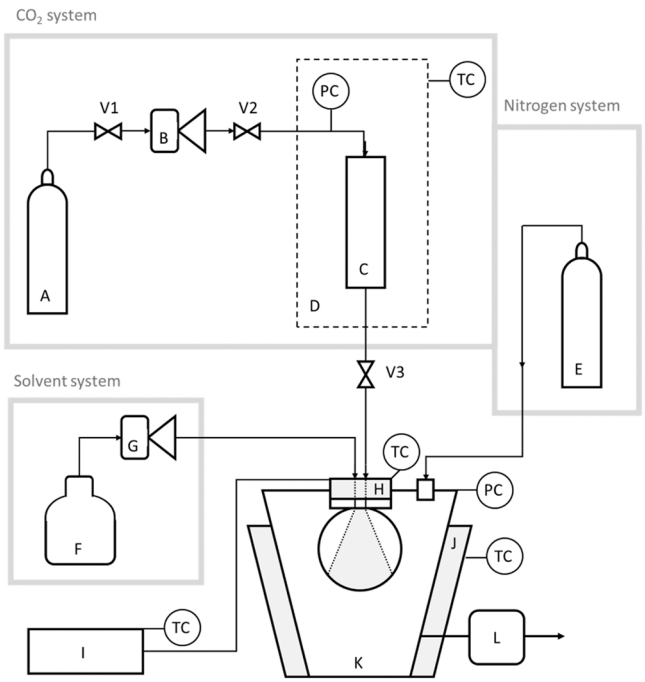

Fig. 1. Schematic diagram of the SASD process featuring two particle isolation strategies used in this work: (1) particle isolation in a filter paper; (2) particle isolation in an aqueous excipient solution. A, CO_2 cylinder; B, cooler and gas compressor; C, CO_2 storage vessel; D, temperature-controlled (TC) water bath; E, compressed nitrogen; F, API solution flask; G, HPLC pump; H, high-pressure nozzle; I, nozzle heater; J, drying chamber heating unit; K, drying chamber; L, Filter; V1,2,3, valves; PC: pressure controlled.

into a suspension. During the reconstitution process of the dried powder, the aqueous-soluble excipient would act as a matrix for the API particles by facilitating their redispersion [28]. Sorbitol has been used in combination with the studied APIs, for instance in commercial oral suspensions of indomethacin (Indocin) [29] and naproxen (Naprosyn) [30], and it is a common excipient used to enhance particle resuspension behaviour of dry powders produced via conventional spray-drying and has been used in intramuscular injections at concentrations up to 25% [31–33]. The main aim is to assess if the SASD process is suitable to produce crystalline API particles for reconstitution into aqueous suspensions.

2. Materials and methods

2.1. Materials

Indomethacin (99% purity) and naproxen (98% purity) were purchased from Baoji Guokang Bio-Technology Co. Ltd. (China). D-Sorbitol (≥98%) was purchased from Sigma Aldrich (Germany). Poloxamer 188 (Kolliphor P 188) and Tween 20 were purchased from Sigma Life Science (Ireland). Acetone (>=99.8%) and methanol (HPLC grade) were purchased from Fisher Chemicals (Ireland). Carbon dioxide (99.98%) was supplied by BOC (Ireland). Purified water was freshly prepared using a Milli-Q Advantage A10 Merck Millipore (Denmark) water purification system.

3. Methods

3.1. Solution preparation

Acetone and methanol were used as solvents. The solvent selection was based on the solubility of the APIs (naproxen and indomethacin) and sorbitol in each solvent. Indomethacin and naproxen are highly soluble in acetone [34,35]. As sorbitol is insoluble in acetone, methanol was selected as a solvent in the experiments where sorbitol was used (DoE experimental runs 9–12, Table 1) [36]. For each experimental run, 400 mg of the API was dissolved in 20 mL of solvent. In the DoE experimental runs 9–12, 400 mg of sorbitol were added to the API methanol solution. The ratio of API:sorbitol was set to 1:1 (w/w) based on previous screening experiments (not included in this manuscript) where higher proportions of sorbitol led to nozzle blocking during supercritical CO_2-assisted spray drying (SASD). The API solution (with/-without sorbitol) was sonicated for 10 min and filtered using a Fisher brand PFTE 0.2 μm filter paper, prior to SASD.

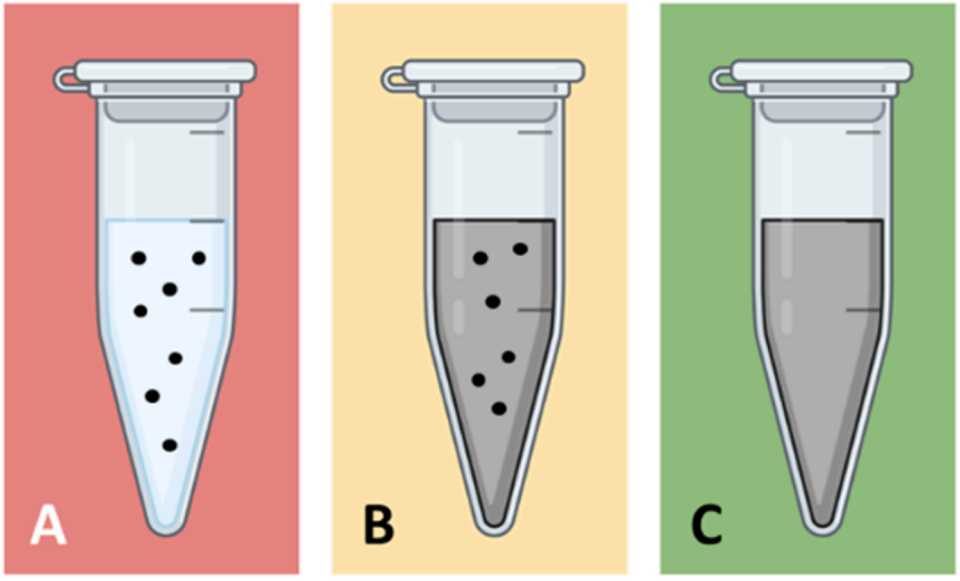

Fig. 2. Colour code visual macroscopic classification and assessment of the resuspension of the SASD samples. A representative example of each case is presented. (A) In red: Homoaggregated particle suspension: Visible particles and transparent media. (B) In yellow: Homoaggregated particle suspension: Visible particles and opaque media. (C) In green: Homogeneous particle suspension. Created with BioRender.com.

3.2. Supercritical CO_2-assisted spray drying (SASD)

Fig. 1 shows the schematic representation of the experimental setup used for supercritical CO_2-assisted spray drying (SASD). It consists of two distinct systems, namely, the solvent and the CO_2 systems, pumped independently into a coaxial nozzle (H in Fig. 1) using a Waters 515 HPLC pump and a Teledyne ISCO 260D pump, respectively. The API solution and the supercritical CO_2 mix and are atomised through a stainless-steel coaxial nozzle with a mixing volume of 0.1 cm^3 (thickness of nozzle disk is 0.5 mm, with 5 ×40 μm orifices array and a cross pattern with 500 μm spacing). The temperature in the nozzle is controlled using a CSi8D benchtop controller and heating resistors (Omega, UK) and maintained at 50 °C. The API solution is atomised into a 1000 cm^3 drying chamber (K in Fig. 1) which is surrounded by a OMEGALUX rope heater (Omega, UK) (J in Fig. 1) which maintains the drying chamber at 50 °C to facilitate evaporation of the organic solvent once the API solution is atomised. A constant flux of nitrogen at room temperature is circulated through the drying chamber from the top. Finally, the spray-dried particles (together with the CO_2, N_2 and organic solvent gaseous feeds) exit the drying chamber.

When the particles exit through the drying chamber (K in Fig. 1) outlet, they are collected in a filter paper. The filter paper traps the API dried particles, while the CO_2, N_2, and solvent vapour pass through it. The particle collection unit (L in Fig. 1) consists of a metal filter and a Whatman 90 mm Cat 1001 090 filter paper (200 nm pore size). The samples were harvested and stored in vials inside a desiccator before characterisation, to prevent the occurrence of polymorphic conversions over time. An anti-static gun was used in the cases where the powders were electrostatic. Later, the ability of the API particles to constitute a homogeneous suspension was explored. In the protocol established, 1 mg of each sample produced by CO_2-assisted spray drying (DoE experimental runs 1–12, Table 1) was added to 1 mL of "Aqueous solution 1″ (0.1% w/v poloxamer 188% and 0.1% w/v Tween 20 solution), or "Aqueous solution 2″ (1% w/v poloxamer 188% and 1% w/v Tween 20 solution). The composition of the aqueous suspensions was selected according to the target application. Poloxamer 188 and Tween 20 are excipients commonly used for parenteral use that stabilise hydrophobic particles [37,38]. Then, the suspension was manually shaken for 30 s. Subsequently, it was assessed macroscopically by placing the vial in front of a black background and illuminating it with a flashlight. If the suspension was determined as homogeneous (Fig. 2C), another 1 mg was added further until macroscopic aggregates appeared, and thus homoaggregation occurred. Homoaggregation was also characterised using optical microscopy as per Fig. S5 in the Supporting information. The homoaggregated samples were classified into two different categories (Fig. 2): a transparent suspension with macroscopic aggregates (Fig. 2A), and an opaque suspension with macroscopic aggregates (Fig. 2B). The objective of this approach was to successfully produce a reconstitutable powder and characterise the successful suspensions.

To isolate the API particles from the excipient aqueous solution and sorbitol, a 10 mL particle suspension was placed in a centrifuge vial and centrifuged for 10 min at 5000 rpm (Eppendorf centrifuge 5810 R, Germany). The supernatant was removed, leaving the sediment at the bottom of the vial. The sediment was resuspended in deionised water, followed by another centrifugation cycle to remove possible residual water-soluble constituents of the suspension (poloxamer 188, Tween 20, and sorbitol), thus, isolating the hydrophobic APIs. Finally, the sediment (API particles) was used for further characterisation.

3.3. Design of experiments (DoE)

A 3-factor 2-level Design of Experiments (DoE) was used to assess the influence of pressure, temperature, type of solvent, and presence of excipient/matrix former (sorbitol) on the particle size and solid form of the API particles produced using the SASD method. The solvents were selected according to the solubility of the APIs (indomethacin, naproxen) and the co-sprayed excipient (sorbitol). Table 1 lists the SASD processing conditions used in this DoE. In the Supporting Information, Fig. S1 presents a schematic of the DoE listed in Table 1. The temperatures of the nozzle and the drying chamber were set at 50 °C, the API concentration was 20 mg/mL (value based on the solubility of the APIs in the organic solvents), and the volume of API solution sprayed was 20 mL. The minimum (10 MPa) and maximum (15 MPa) values for the pressure were selected in accordance with the limits of the SASD equipment used and the minimum pressure required to ensure having CO2 in the supercritical state [22,39]. The API:sorbitol ratio was established as 1:1 (w/w). Preliminary experiments (not presented in this manuscript) using higher sorbitol concentrations led to nozzle clogging.

3.4. Solid-state characterisation and particle size analysis

3.4.1. X-ray powder diffraction (XRPD)

X-Ray Powder Diffraction (XRPD) in reflection mode was performed at ambient conditions using an X′ Pert PRO MPD XRPD (PANalytical, Philips, Germany) and an Empyrean diffractometer (PANalytical, Philips, Germany), both equipped with Cu-α radiation ($\lambda = 1.5406$ Å) at a voltage of 45 kV, and a current of 40 mA. The instruments were operated in the continuous scan mode and the samples were analysed in the angular range 4–35° (2θ) with a step size of 0.013° (2θ) and a measuring time per step of 18.87 s

3.4.2. Fourier-transform infrared spectroscopy (FT-IR)

The Fourier-Transform Infrared Spectroscopy (FT-IR) spectrum of the samples produced with SASD was measured at ambient temperature using the Nicolet iS50 FT-IR spectrometer (Thermo Fisher Scientific, USA). Approximately 5–10 mg of the samples were spread on a crystal with a pushing arm. Each spectrum was collected at wavelengths ranging from 4000 cm^{-1} to 400 cm^{-1} using an attenuated total reflection (ATR) accessory for the analysis of powders, and 64 scans were collected for each sample with a resolution of 4 cm^{-1}.

3.4.3. Differential scanning calorimetry (DSC)

Differential Scanning Calorimetry (DSC) was performed using a Netzsch Polyma 214 DSC (Netzsch, Germany) that was calibrated using Sn (Tin) as a reference. Samples (5–10 mg) were crimped in non-hermetic aluminium pans (25 μl) and scanned at a heating rate of 10 °C/min from 25 °C to 200 °C (above the melting temperatures of indomethacin and naproxen) under a nitrogen purge of 50 mL/min. The instrument was equipped with a refrigerated cooling system. The samples were stored in a desiccator and the DSC analyses were performed 2 weeks after producing the CO_2-assisted spray-dried powdered samples where the solid stability of the powder was also studied. The physical mixtures containing sorbitol and API mixtures were prepared by gentle grinding using a mortar and pestle for a short period (~ 2 min).

3.4.4. Scanning electron microscopy (SEM)

The SU70 Hitachi and Carryscope JEOL (Hitachi, Japan) SEM instruments were used to take images of the particles collected in a filter. Each sample was carefully placed on a carbon tape previously stuck to an SEM 15 mm stub. Then, it was coated with a gold deposit using an Emitech K550 (Emitech, UK) instrument at 20 mA and for 2 min. The samples were imaged in field-free mode at a voltage of 10 kV and a working distance of 10 mm. At least 10 images were taken to verify the uniformity of the samples. The average particle sizes were measured using the Image J software. A minimum of 100 particles per sample were measured to assess particle size.

3.5. Process yield

The process yield was defined as the amount of powder collected in the filter relative to the amount of solid dissolved in the feed solution (Eq. 1).

Table 2
List of solid forms and average particle sizes obtained for indomethacin and naproxen produced by SASD. The solid-state of the samples was analysed by XRPD and the particle sizes were measured by SEM. The yield obtained for each experiment was calculated according to Section 2.2.6.

DoE Experimental run	Indomethacin			Naproxen		
	Solid-state	Particle size (μm)	Yield (%)	Solid-state	Particle size (μm)	Yield (%)
1	Amorphous	1.43 ± 0.80[a]	11.1	Form 1	1.13 ± 0.61	7.7
2	Amorphous	0.81 ± 0.39	29.7	Form 1	0.44 ± 0.27[a]	22.3
3	Amorphous	0.88 ± 0.51	5.0	Form 1	0.77 ± 0.51	13.6
4	Amorphous	1.30 ± 0.89[a]	3.9	Form 1	1.16 ± 0.57	1.6
5	Amorphous	2.58 ± 2.95[a]	9.1	Form 1	1.73 ± 1.11[a] / 1.41 ± 1.03[c]	10.3
6	Amorphous	1.36 ± 0.95	8.1	Form 1	0.80 ± 0.49[a]	6.0
7	Amorphous	1.73 ± 0.93	5.4	Form 1	0.69 ± 0.33	2.6
8	Amorphous	2.09 ± 1.63[a]	19.1	Form 1	1.34 ± 0.83[a] / 1.48 ± 1.20[c]	19.2
9	α + γ[b]	6.86 ± 5.23[a]	5.8	Form 1	3.22 ± 1.37[a] / 1.55 ± 0.87[c]	13.0
10	α + γ[b]	1.51 ± 1.03[a]	22.8	Form 1	1.24 ± 0.89[a]	12.3
11	α + γ[b]	4.06 ± 4.85[a]	5.4	Form 1	1.39 ± 0.82[a]	14.7
12	α + γ[b]	7.59 ± 4.29[a]	10.5	Form 1	3.19 ± 1.76[a] / 2.00 ± 1.30[c]	28.0

a Particles presented irregular morphologies and/or particles aggregates/agglommerates.
[b] A significant amorphous halo was observed in the XRPD patterns (Fig. 3).
[C] Particle size measured after resuspension/reconstitution as per Section 2.2.3.

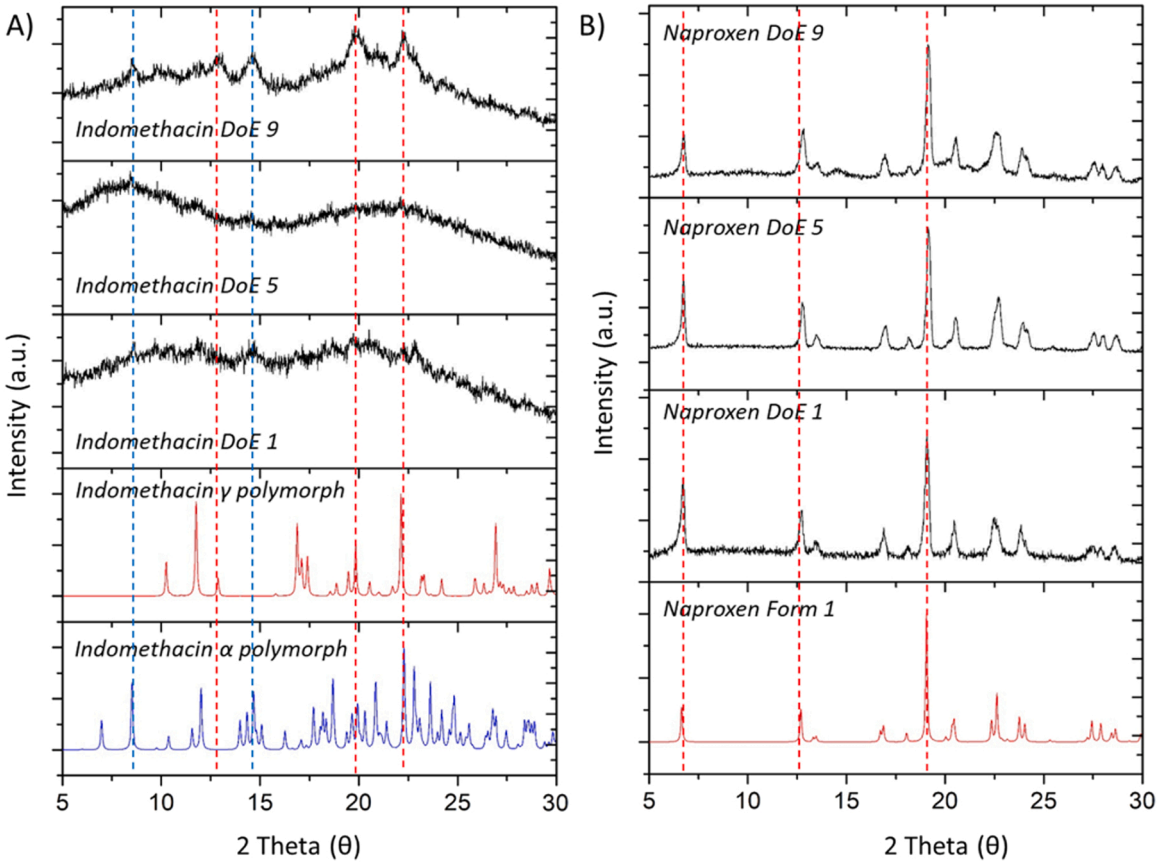

Fig. 3. XRPD patterns of representative samples obtained from the DoE approach produced by SASD as per Table 1 of the API sprayed using methanol as solvent (DoE experimental run 1), acetone as solvent (DoE experimental run 5), and methanol as solvent co-sprayed with sorbitol (DoE experimental run 9). The theoretical XRPD for naproxen (Form 1) and indomethacin (forms α and γ) forms from the CSD are presented as references. All XRPD patterns for the samples obtained for DoE experimental runs 1–12 are presented in Fig. S4 in the Supporting Information. For indomethacin, blue dotted lines indicate characteristic peaks of the α form at 8.5° and 14.7° 2θ, while red dotted lines indicate characteristic peaks of the γ form at 12.9°, 19.8° and 22.1° 2θ. For naproxen, red dotted lines indicate characteristic peaks of form 1 at 6.6°, 12.7°, and 19.1° 2θ.

$$\frac{API \quad product(mg)}{API \quad feed \quad concentration(mg/ml) \times Sprayed \quad volume \quad (ml)} \times 100 \tag{1}$$

3.6. Solubility calculations using COSMO-RS

COSMO-RS calculations were conducted to estimate the solubility/miscibility of each API (indomethacin, naproxen) in sorbitol. The molecules were taken from the COSMObase dataset (COSMObase2021) and the calculations were carried out using COSMOtherm2021 [40,41]. All calculations were performed on a TZVPD level using all conformations

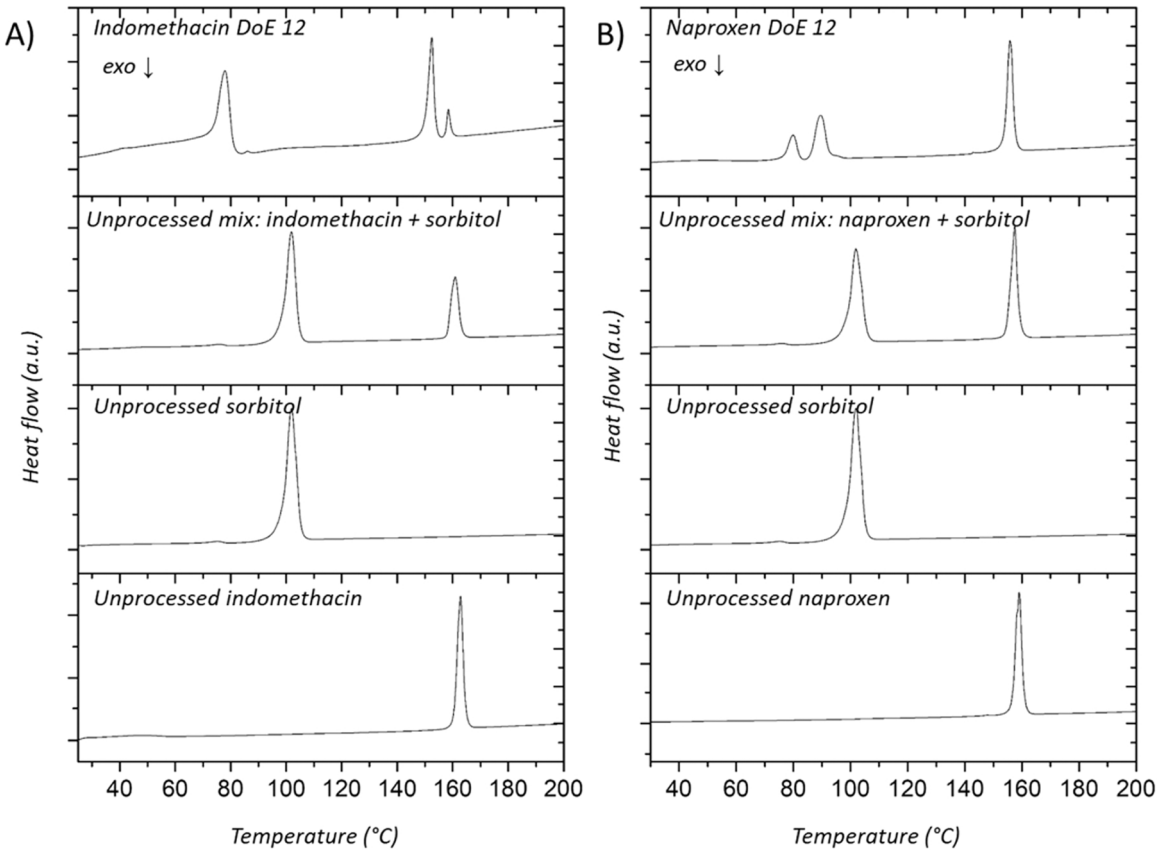

Fig. 4. DSC analysis of: A) Unprocessed indomethacin, unprocessed sorbitol, mixture (mix) of unprocessed naproxen and sorbitol, supercritical CO_2-assisted spray dried indomethacin with sorbitol using the conditions of DoE experimental run 12; B) Unprocessed naproxen, unprocessed sorbitol, mixture (mix) of unprocessed naproxen and sorbitol, CO_2-assisted spray-dried naproxen with sorbitol using the conditions of DoE experimental run 12. The samples' peak melting points, onset temperatures, and the enthalpies of fusion for these thermograms are listed in Tables S1 and S2 in the Supporting Information.

of the molecules retrieved from the database (naproxen 4 conformations, indomethacin: 11 conformations, and sorbitol 28 conformations). For the lattice energy calculations, the COSMO-RS reference framework was used (the reference state of the calculation is 1 bar (0.1 MPa) of an ideal gas and 1 mol of solvent, see Biovia COSMOtherm 2021 reference manual [42–44].

4. Results and discussion

4.1. Supercritical CO_2-assisted spray drying of indomethacin and naproxen with/without sorbitol followed by particle collection in a filter

4.1.1. Particle size and solid-state analysis

The solid form and particle size of the API (naproxen, indomethacin) particles produced using the SASD method and isolated in a filter (L in Fig. 1) were analysed to assess the impact of the processing conditions (pressure and flow rate), solvent type (acetone, methanol) and presence of an excipient (sorbitol). XRPD was used to study the solid form of the samples produced by SASD, and these were compared with the polymorphic forms of each API reported in the literature and the theoretical XRPD patterns available in the Cambridge Structural Database (CSD). The reference patterns extracted from the CSD were COYRUD for Form 1 of naproxen, and INDMET02 and INDMET03 for the α and γ polymorphs of indomethacin, respectively. The patterns from the CSD were selected taking into consideration the experimental results. Residual impurities from other polymorphic forms reported in the literature were not observed.

The particle size of the samples was assessed using SEM despite the particles presenting irregular morphologies and particle aggregates/agglomerates (Figs. S2 and S3 in the Supporting Information), providing an estimation of the average particle size of the samples. However, the impact of the processing conditions on the particle size could not be studied in detail due to uncertainties associated with this method.

Table 2 lists the resulting solid forms and particle sizes obtained for all APIs (naproxen, indomethacin) samples produced by the SASD method using the DoE approach (as per processing conditions listed in Table 1). XRPD analysis showed that naproxen particles produced by SASD, in the presence or absence of sorbitol, presented Form 1 (stable form) consistently throughout all the experiments (Fig. 3B). It is important to note that XRPD analysis of the samples was conducted within 24 h after the powders were collected from the CO_2-assisted spray dryer, and no crystallinity related to sorbitol was observed. On the other hand, samples produced using the conditions of the SASD experimental runs using indomethacin in the absence of sorbitol (DoE experimental runs 1–8, in Tables 1 and 2), amorphous particles were obtained. For SASD samples produced in experimental runs where indomethacin and sorbitol were dissolved together in methanol and co-sprayed (DoE experimental runs 9–12 in Tables 1 and 2), the XRPD patterns revealed a strong amorphous halo pattern with some crystallinity. The peaks observed in the XRPD patterns did not present good resolution, but identifiable peaks were attributed to a mixture of the α and γ polymorphs of indomethacin (Fig. 3 A).

The measured average particle size for indomethacin and naproxen particles produced in the absence of sorbitol (DoE experimental runs 1–9 in Tables 1 and 2) ranged between 0.81 and 2.85 μm and 0.44–1.73 μm, respectively (measured by SEM, presented in Figs. S2 and S3 in the Supporting Information). Contrarily, when sorbitol was used, the average particle size range for indomethacin was 1.51–6.86 μm, and for

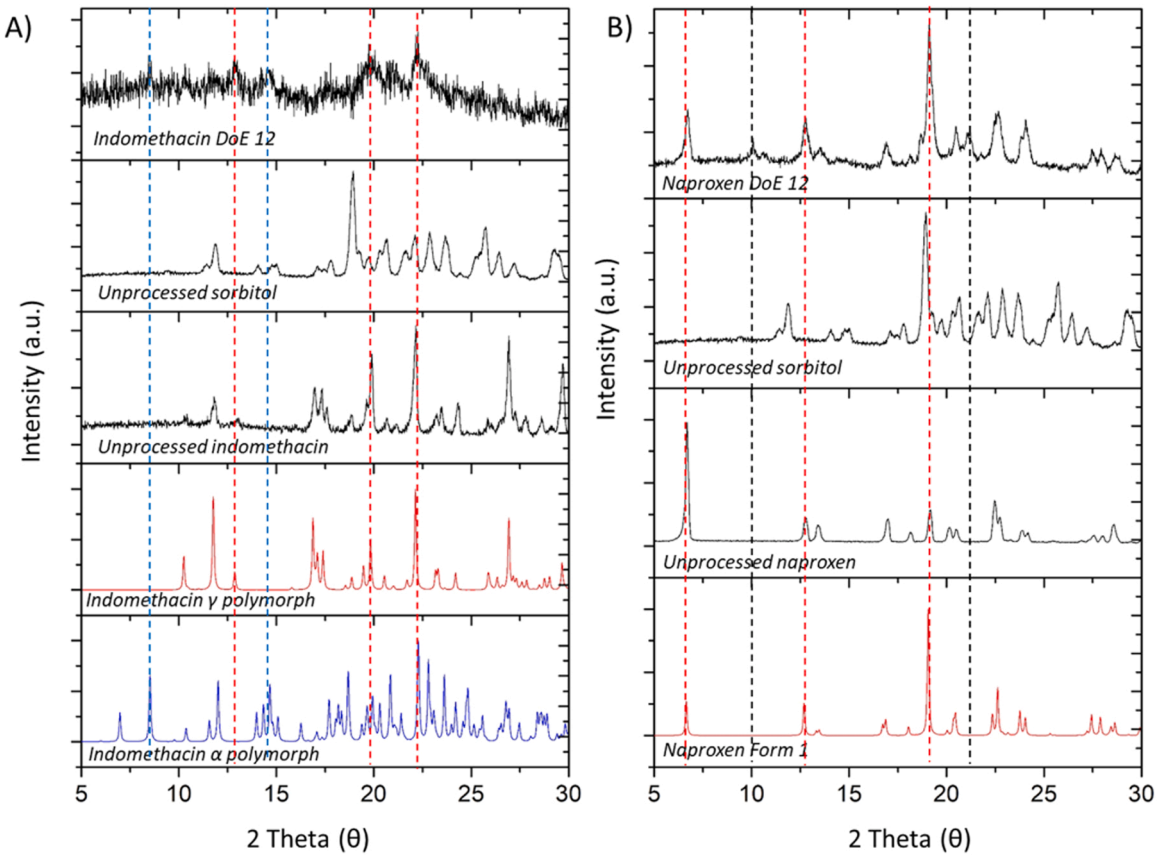

Fig. 5. Additional XRPD patterns of indomethacin and naproxen were performed immediately before the DSC measurements (2 weeks after production) to study the solid stability of the samples. Immediately after XRPD, these samples were analysed by DSC, as presented in Fig. 4. Theoretical XRPD patterns for the α and γ polymorphs of indomethacin (INDMET02 and INDEMT03), and Form 1 (COYRUD) of naproxen were used from the CSD. For indomethacin, blue dotted lines indicate the characteristic peaks of the α polymorph at 8.5° and 14.7° 2θ, while the red dotted lines indicate the characteristic peak of the γ polymorph at 12.9°, 19.8°, and 22.1° 2θ. For naproxen, the red dotted lines indicate the peaks of Form 1 at 6.6°, 12.7°, and 19.1° 2θ. The black dotted lines indicate peaks corresponding to sorbitol solid forms reported by DeJong and Hartel [51].

Table 3
Calculation of the lattice energy ($\Delta G_{lattice}$) of indomethacin and naproxen by adding the free energy of solvation ($\Delta G_{solvation}$) calculated using COSMO, and the free energy of crystallisation ($\Delta G_{crystallisation}$) calculated using Eq. (2).

Naproxen Solvent	Experimental solubility (molar fraction)[a]	$\Delta G_{crystallisation}$ (kJ/mol)	$\Delta G_{solvation}$ (kJ/mol)	$\Delta G_{lattice}$ (kJ/mol)
EtOAc	0.0263	8.87	53.65	62.66
Acetone	0.0504	7.24	54.01	61.41
Dichloromethane	0.0155	6.60	44.78	55.08
Acetonitrile	0.0064	12.07	47.34	59.85
Methanol	0.0122	10.91	48.90	59.82
Indomethacin				
Acetonitrile	0.0021	14.71	68.18	82.89
Ethanol	0.0027	14.15	71.73	85.79
Methanol	0.0021	14.73	70.50	85.24
EtOAc	0.0093	11.03	76.48	87.52
Acetone	0.0234	9.30	76.72	86.01

[a]Experimental solubility of naproxen and indomethacin in various organic solvents in mole fraction was extracted from the literature [34–36,53]

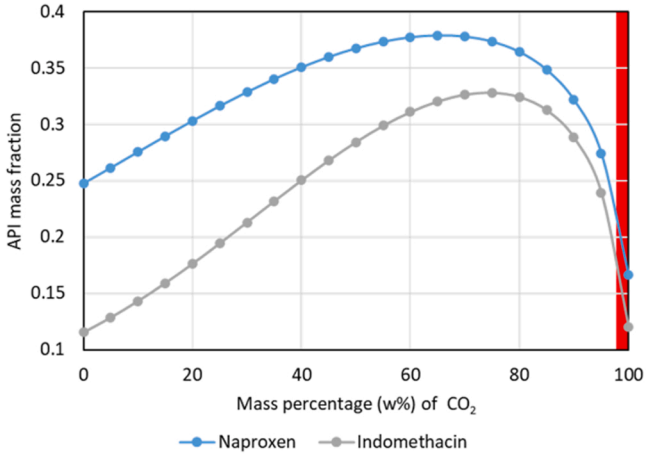

Fig. 6. Solubilities (in mass fraction) of indomethacin and naproxen (API concentration at 20 mg/mL) in sorbitol (20 mg/mL) and methanol in liquid CO_2 at 50 °C calculated using COSMO, as per section 2.2.7. The experimental conditions used in the work presented herein are highlighted in red.

naproxen was 1.24–3.22 μm. For both APIs, samples produced using the SASD processing conditions of experimental runs 9 and 12 presented an increment in the average particle size that was attributed to sorbitol forming a matrix surrounding the API particles. As previously stated, due to a non-uniform particle morphology, the particle size could not be studied in further detail.

The collection yield for both APIs in these experiments was typically below 30% due to the instrumental set up. Higher yields have been reported when e.g. a product was isolated using a cyclone [17,18,45–47]. Moura et al. used a high-efficiency cyclone as the particle collection system in SASD and obtained yields ranging from 50% to 70% [18]. The adhesion of particles, particularly sub-micron and nano-sized particles,

Table 4
Calculation of the API mass fraction solubilities (naproxen, indomethacin) in the liquid mixture composed of CO_2, methanol, and sorbitol at 50 °C for the DoE experimental runs 9–12.

DoE experimental run	APIs (naproxen and indomethacin) mass fraction × 1000	Solubility (mass fraction)	
		Naproxen	Indomethacin
9	0.0797	0.178757	0.13900
10	0.0499	0.174231	0.134214
11	0.1984	0.194097	0.155223
12	0.3158	0.208159	0.170629

to the walls of drying chambers often leads to low collection yields [17].

4.1.2. Thermal analysis

To provide insight on the effect of co-spraying sorbitol with each model API (naproxen, indomethacin) using SASD, the thermal properties of a representative sample of each API processed by this method (DoE point 12), together with unprocessed APIs and sorbitol, were analysed using DSC. The DSC data is detailed in Tables S1 and S2 in the Supporting Information. It is important to remark that the samples were analysed with DSC 2 weeks after production, and XRPD was conducted again to assess any possible changes in the solid form of the samples. The powder produced using the conditions of DoE experimental run 12 was selected as the representative sample for analysis due to two reasons. First, it was conducted at a high flow rate (0.4 mL/min) and thus, was time efficient. Second, it used a pressure of 10 MPa instead of 15 MPa resulting in less supercritical fluid consumed throughout the process and thus, cost-effective.

Fig. 4A shows that unprocessed indomethacin presented an onset temperature of 160.5 °C. The melting temperature of the γ form of indomethacin has been reported to be in the range of 158–161 °C, therefore, as also is observed in the XRPD pattern presented in Fig. 5 A, unprocessed indomethacin corresponds to the γ polymorph [35,48].

Fig. 4B shows that unprocessed naproxen presents an endothermic peak with a peak temperature of 159.0 °C that corresponds to Form 1. Song et al. reported the melting peaks of all reported polymorphic forms of naproxen (Forms 1, 2, 3, and 4), and Form 1 presented the melting peak at the highest temperature (156.2 °C) while, for instance, Form 4 presented an endothermic peak at the second highest temperature at 148.2 °C [49]. The XRPD pattern of unprocessed naproxen supported the conclusion that it corresponds to Form 1 (Fig. 5B). Nevertheless, the onset temperature (i.e. intersection point of the extrapolated baseline and the inflectional tangent at the beginning of the melting peak) was considered of more relevance to determine the melting temperature as it indicates the start of the melting event and it is more independent to sample mass and heat rate compared to the melting peak.

Unprocessed sorbitol (displayed in Figs. 4A and 4B for comparison purposes) presented an endothermic melting peak with an onset temperature of 98.5 °C. The onset temperature coincided with the γ polymorph of sorbitol reported by Nezzal et al. at 96 °C (the highest onset temperature for all the polymorphs reported) [50]. Moreover, the XRPD pattern for sorbitol (Fig. 5) also matched with the XRPD pattern of the γ polymorph of sorbitol reported by DeJong and Hartel [51]. Tables S1

Table 5
Results of the resuspension studies. The colour code classification is detailed in Fig. 2. For the homogeneous particle suspensions, the maximum concentration reached is defined. (A) In red: Homoaggregated particle suspension: Visible particles in transparent solution. (B) In yellow: Homoagreggated particle suspension: Visible particles in opaque solution. (C) In green: Homogeneous particle suspension.DoE experimental run.

DoE experimental run	Indomethacin		Naproxen	
	Aqueous solution 1 [a]	Aqueous solution 2 [b]	Aqueous solution 1 [a]	Aqueous solution 2 [b]
1	A	A	B	B
2	A	A	B	B
3	A	A	B	B
4	A	A	A	A
5	A	A	B	C (1 mg/mL) [c]
6	A	A	B	A
7	A	A	B	A
8	A	A	B	B
9	A	A	C (5-6 mg/mL) [c]	C (5-6 mg/mL) [c]
10	A	A	C (1-2 mg/mL) [c]	C (1-2 mg/mL) [c]
11	A	A	B	B
12	A	A	C (4-5 mg/mL) [c]	C (4-5 mg/mL) [c]

a Poloxamer 188 0.1% w/v, Tween 20 0.1% w/v
b Poloxamer 188 1% w/v, Tween 20 1% w/v
c Maximum concentration achieved before forming a homoagreggated particle suspension; visible particles in opaque solution

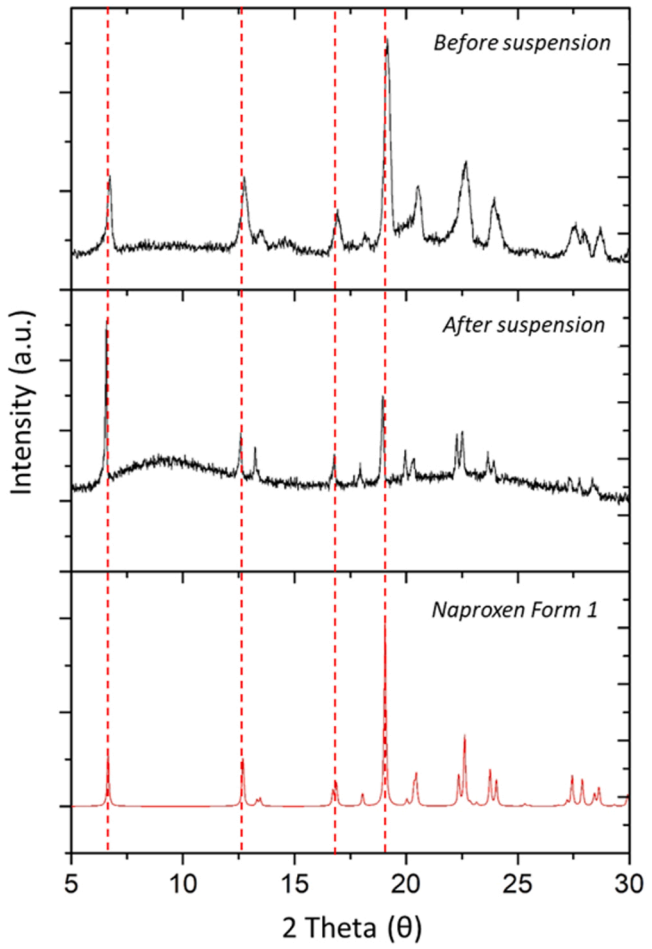

Fig. 7. XRPD patterns of SASD-processed naproxen powder before suspension, and the isolated naproxen particles after suspension (according to section 2.2.3). The representative sample used was produced using the conditions of DoE experimental run 12 for naproxen, at a concentration of 1 mg/mL in an aqueous solution containing poloxamer 188 (0.1% w/v) and Tween 20 (0.1% w/v). The red dotted lines indicate the peaks of Form 1 at 6.6°, 12.7°, 16.8° and 19.1° 2θ. The black dotted lines indicate peaks corresponding to sorbitol.

and S1 in the Supporting Information list the DSC data of the thermograms shown in Fig. 4.

There was no evidence of eutectic phase formation, based on thermal analysis of the physical mixtures of unprocessed APIs and sorbitol samples [52].

The DSC curves for the SASD-processed powders differed from the unprocessed physical mixtures. For the indomethacin sample produced using the conditions of DoE experimental run 12 (co-sprayed indomethacin and sorbitol, Fig. 4A), sorbitol presented one peak in the DSC thermogram. The peak with an onset temperature of 73.7 °C was attributed to the E subform of sorbitol [50]. Regarding indomethacin, it presented two distinguished peaks with onset temperatures at 149.9 and 157.3 °C that corresponded to the α and γ polymorphs of indomethacin, respectively [35,48]. The α form of indomethacin presents a melting temperature in the range of 149–154 °C as reported in the literature [35,48]. The appearance of these different polymorphs of indomethacin might have been heat-induced during the DSC, or both polymorphs may have been present in the analysed sample as the XRPD pattern of the same sample (Fig. 5 A) analysed before DSC presented an amorphous halo with traces of crystallinity. The conclusion from the DSC and XRPD results was that SASD impacted the crystallinity of the sample, as the nucleation of different polymorphs of indomethacin may have occurred. This might have been due to the fast nucleation events during SASD processing which did not allow the kinetic crystallisation of indomethacin. Other possible causes might rely on the processing conditions (temperature, pressure, flow rate) that were not adequate for the crystallisation of a single form.

The naproxen sample produced in the DoE experimental run 12 presented a peak with an onset temperature of 153.8 °C corresponded to Form 1 of naproxen, as previously discussed and as observed in the XRPD pattern (Fig. 5B). Nevertheless, sorbitol presented two separate melting peaks at 79.9 °C and 89.5 °C (onset temperatures of 76.6 °C and 86.1 °C) in that sample that were attributed to the E subform and α polymorph of sorbitol, respectively, by comparing them to the reported data by Nezzal et al. [50]. The XRPD analysis conducted immediately before DSC (Fig. 5B) revealed two additional peaks at 10.1 and 21.2 2θ compared to the XRPD patterns after particle production (Fig. S4, Supporting Information) that were attributed to sorbitol crystalising to the aforementioned solid forms during storage. Therefore, sorbitol might have been initially presented in an amorphous, semicrystalline, or nanocrystalline solid state that after two weeks crystallised upon storage. It is important to remark that the samples were stored in a desiccator to prevent recrystallisation, however, as previously observed, sorbitol presents a complex polymorphic behaviour [50]. On the other hand, naproxen did not present changes in the solid form, as Form 1 is the most stable polymorph.

To sum up, the APIs and sorbitol powders processed by SASD presented thermal properties that contrasted with the unprocessed solid mixtures. Consequently, SASD processing had an impact on the physicochemical properties of the resulting powders leading to complex behaviours of sorbitol. Naproxen samples consistently presented the most stable polymorphic form (Form 1) while all indomethacin samples presented amorphous powders, with some crystallinity only in the samples produced using the conditions of DoE experimental runs 9–12 where sorbitol was co-sprayed.

4.2. Solubility modelling of the APIs in sorbitol and CO_2

To further explore the interactions of the APIs with sorbitol, COSMO-RS modelling was used to calculate the solubility of the APIs in sorbitol, as per section 2.2.7. To estimate the solubility of naproxen and indomethacin in sorbitol, the concept of lattice energy was used. The lattice energy ($\Delta G_{lattice}$), defined as the difference in free energy between the crystalline state and the gas state can be obtained by summing the free energy of solvation ($\Delta G_{solvation}$, obtained using COSMO as per section 2.2.7) and the free energy of crystallization ($\Delta G_{crystallisation}$, obtained from experimental solubility data using the Van 't Hoff equation, Eq. 2).

$$\Delta G_{lattice} = \Delta G_{solvation} + \Delta G_{crystallisation} = \Delta G_{solvation} + RT \quad \ln(x) \qquad \text{Eq. 2}$$

The input values of the components (indomethacin γ polymorph, naproxen Form 1 and, D-sorbitol) solubilities in diverse organic solvents were extracted from the literature [34–36,53]. The results of the calculations are given in Table 3.

Using the mean lattice energies and the calculated solvation energies in a 1:1 API:sorbitol (w/w) mixture as per Section 2.2.1, the solubility of naproxen and indomethacin in sorbitol was calculated. The solubility in mass fraction of indomethacin and naproxen in sorbitol was 0.00042 and 0.0029, respectively. From these calculations, it can be concluded that both naproxen and indomethacin have quite low solubility in sorbitol, and hence, from a thermodynamic perspective, the APIs could crystallise from an API:sorbitol 1:1 (w/w) mixture. However, as observed in the previous section, despite indomethacin being able to crystallise in thermodynamic terms, it was not possible in kinetic terms due to the fast evaporation of the solvent mixture, and thus trapping indomethacin in an amorphous state. Conversely, the calculations obtained agree with naproxen where the crystallisation of the most stable form (Form 1) occurred in thermodynamically and kinetically terms during spray drying. Additionally, due to the low solubilities of the APIs

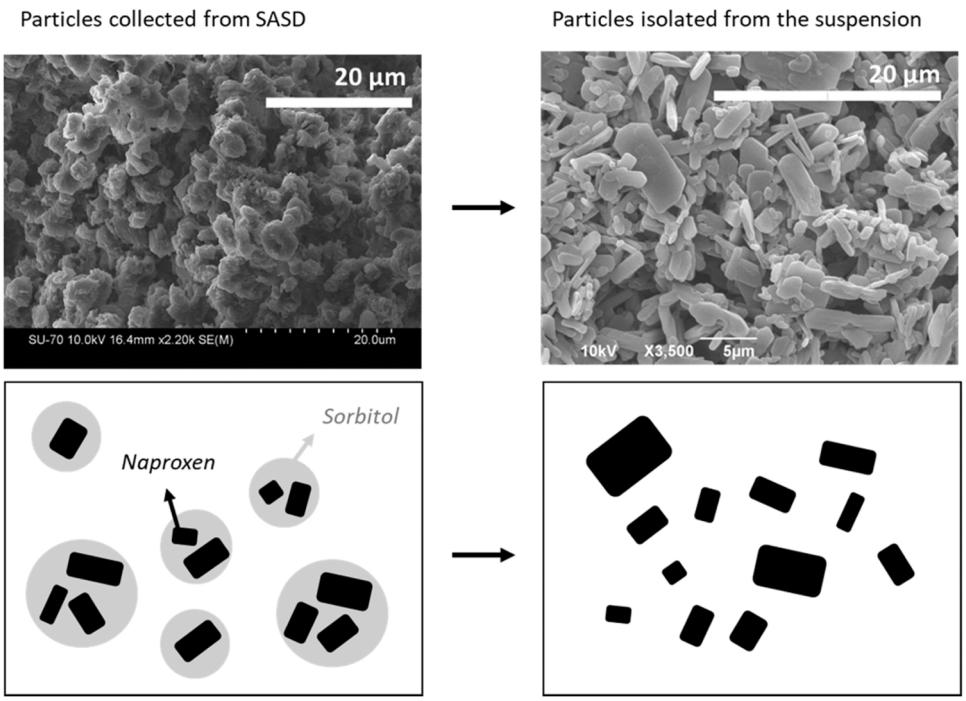

Fig. 8. Schematic representation and SEM images of the naproxen particles produced using the conditions of DoE experimental run 12 (co-sprayed with sorbitol) before suspension (left) and after resuspension (right).

in sorbitol, it is expected that sorbitol, initially present in the amorphous phase, could crystallise during storage, as there is no evidence of eutectic phases (see Section 3.1.2). Thus, the modelling supported the experimental conclusions obtained from the thermal analysis.

To assess the influence of CO_2 on the solubility of naproxen and indomethacin, COSMO calculations were carried out assuming methanol, sorbitol and CO_2 to be hypothetical liquids instead of a supercritical mixture. The solubility of the APIs was calculated at 50 °C (nozzle temperature used in the experiments) using the experimental solubility of the APIs at 25 °C in pure methanol (Fig. S6 Supporting Information). The solubilities of the APIs in methanol were used as starting point (calibration) for the COSMO calculations. The solubilities in mass fractions of indomethacin and naproxen at 25 °C in methanol are 0.02488 and 0.08152 [53].

The results as per Fig. 6 indicate that there is a strong synergistic effect between sorbitol, methanol and CO_2 at 50 °C. The solubility of the APIs increases in the system as CO_2 is added until it reaches a maximum and then, dramatically decreases. At the dramatic decrease (highlighted in red in Fig. 6) is where the DoE experimental runs were conducted. The solubility of all components in the mixtures used in DoE experimental runs 9–12 (see Table 1) was calculated and is shown in Table 4.

These results show that in all cases for DoE experimental runs 9–12, all components (e.g. naproxen, indomethacin, sorbitol) are dissolved in liquid CO_2. According to the modelling conducted, any crystallization of the APIs (naproxen and indomethacin) is expected to happen after exiting the nozzle when the solvent evaporates inducing the precipitation of the API particles. This agrees with the experimental observations where no nozzle clogging was observed. It is important to take into account that the modelling was conducted considering CO_2 as a hypothetical liquid, and therefore, it presents limitations. To model supercritical CO_2, it has to be considered that CO_2 is compressible like a gas and has solvating properties and similar densities as a liquid [54]. Accurate predictions of the solubilities would require adaptations of the COSMO model [55]. For the purposes of the work presented herein, the calculations conducted sufficed and supported the experimental observations.

4.3. Reconstitution of Sorbitol-Coated Indomethacin and Naproxen Particles Produced by CO_2-Assisted Spray Drying and Collected in a Filter

4.3.1. Suspension Screening

The goal of co-spraying the APIs (naproxen and indomethacin) with sorbitol using the SASD technique was to use sorbitol as a matrix for the crystalline API particles and to create particles with enhanced resuspension behaviour. Once the API particles are mixed with the aqueous dispersant, the sorbitol matrix would easily dissolve in the solution due to its high aqueous solubility, and the API particles would be released and easily resuspended.

The powders produced with the SASD method were suspended in an aqueous solution of poloxamer 188 (polymeric excipient) and Tween 20 (surfactant). Both excipients have been used/reported in the literature for the preparation of parenteral particle suspensions [56,57]. Two different concentrations of the excipients were explored: 0.1% w/v and 1% w/v. The suspensions produced were macroscopically assessed and they were classified into 3 categories, as described in Fig. 2. The objective was to obtain a homogeneous particle suspension free of agglomerates. Nevertheless, in some cases, the particles homoaggregated and were classified into 2 different categories depending on the opacity of the suspension: visible particles in opaque media, and visible particles in transparent media.

Indomethacin samples produced with the SASD method could not constitute a homogeneous particle suspension free of aggregates (Table 5). In all cases for indomethacin, homoaggregates were formed and the media was transparent. The excipient system failed during the resuspension process to replace the solid-air interface with a solid-liquid interface leading to the formation of homoaggregates. The high surface energy of the amorphous indomethacin particles was not possible to be stabilised with the selected excipients, and the only way to reduce it was through the formation of homoaggregates of the hydrophobic particles.

On the other hand, naproxen samples produced using SASD presented improved resuspension behaviour compared to indomethacin. Moreover, naproxen powders made according to the DoE experimental runs 9–12, where sorbitol was used as an excipient, showed enhanced suspension behaviour (Table 5). This fact agrees with the strategy

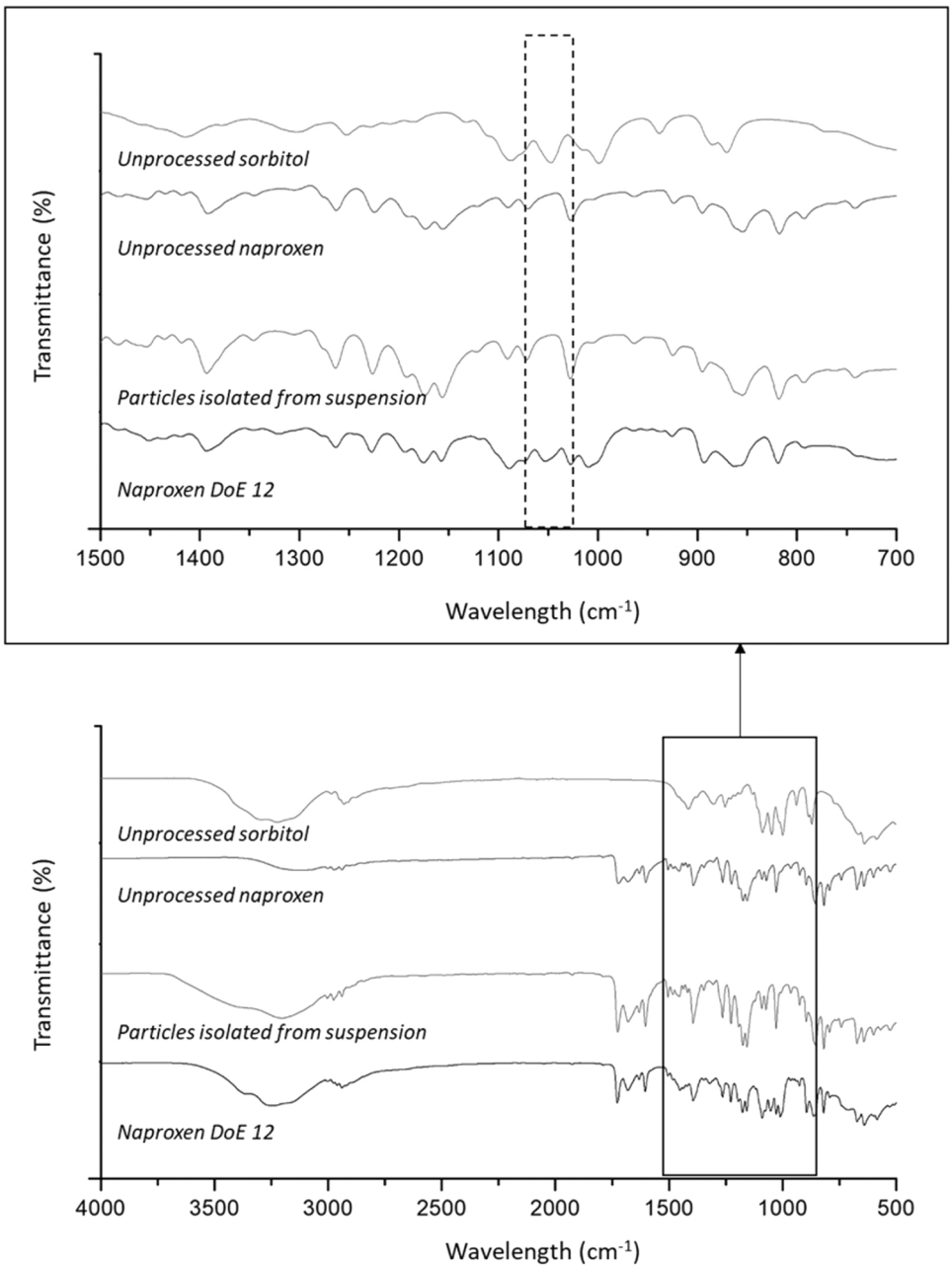

Fig. 9. FT-IR spectra of unprocessed sorbitol, unprocessed naproxen, naproxen produced from the SASD-process ("Nanproxen DoE 12"), and naproxen isolated from suspension ("Particles isolated from suspension").

initially formulated of using this excipient as a matrix to enhance the resuspension behaviour.

It is important to remark that this was a macroscopic assessment of the resuspendability of the SASD-processed API particles. This screening was conducted to select the optimal SASD processing conditions to produce a successful powder for resuspension. Co-spraying of sorbitol was the only condition that enhanced the resuspension behaviour of the SASD-processed naproxen samples. Indomethacin did aggregate upon contact with the aqueous solution, and thus did not present desired properties for an injectable formulation. After the macroscopic evaluation, the particle size and morphology of the successful candidates were studied in detail in the following section.

4.3.2. Suspension characterisation

Taking into consideration the results from the previous section, indomethacin was excluded from further analysis, and the study was focused on naproxen. The samples produced using the conditions of DoE experimental runs 5, 8, 9, and 12 for naproxen were selected according to the previous screening (Table 5). Despite the sample produced using the conditions of DoE experimental run 8 was the only one that was not homogeneous and presented homoaggregates (visible particles in opaque solution), the sample was selected to assess the impact of the different flow rates used in the DoE on the resuspended particle size and morphology. The API particles in the sorbitol matrix might have been impacted by the flow rate. For instance, Moura et al. concluded in the optimisation of SASD that the lower the flow rate, the smaller the particle size, therefore this parameter was worth studying in more detail [18]. The pressure was not studied due to the poor resuspension behaviour of powders produced in the DoE experimental runs 4, 6, and 7 (homoaggregated particle suspensions with visible particles in transparent solution). A naproxen suspension (1 mg/mL) was produced for the selected experimental samples (DoE experimental runs 5, 8, 9, and

12). The particles were then isolated from the suspension and analysed by XRPD. In all cases, the crystal form remained the same. The polymorphic Form 1 of naproxen, as that of the SASD processed powder, was retained in the suspended particles (Fig. 7).

SEM was used to analyse the morphology and particle size of the resuspended particles. The particle sizes obtained for naproxen particles isolated from the suspensions for the samples produced using the conditions of DoE experimental runs 5, 8, 9, and 12, were 1.41 ± 1.03 μm, 1.48 ± 1.20 μm, 1.55 ± 0.87 μm, 2.00 ± 1.30 μm, respectively as per Table 2. The average particle size remained similar for naproxen particles produced using the conditions of DoE experimental runs 5 and 8 before and after resuspension with a change lower than 0.3 μm (see Table 2). Conversely, samples produced using the conditions of DoE experimental runs 9 and 12, where naproxen was co-sprayed with sorbitol, had a different particle size before and after suspension. The average particle size decreased by more than 1 μm after resuspension for both samples (see Table 2). Also, the morphology of the particles changed drastically. The matrix of sorbitol containing the naproxen particles produced using SASD dissolved upon contact with the aqueous solution reducing the particle size and releasing the API particles. This hypothesis was supported by the SEM images. As can be observed in Fig. 8, the morphology of the particles before and after suspension was significantly different. Recrystallisation of the naproxen particles is not likely to have occurred due to the low solubility of the API particles in water, and the fast process of isolation of particles from suspension (Section 2.2.2). Moreover, an experiment spraying sorbitol alone using the conditions of DoE 12 was conducted, but no sorbitol particles were produced. A sticky mass was instead collected in the filter paper. Therefore, naproxen and sorbitol particles would not have formed separately, and the hypothesis of a sorbitol matrix was supported.

A correlation between the particle size after resuspension and the solution flow rate used during the SASD was considered as the size of the API particles in the sorbitol matrix might be dependent on the flow rate, however, no correlation was observed.

FT-IR was performed to determine if sorbitol was fully dissolved when the powder was resuspended. Fig. 9 presents the FT-IR spectra of unprocessed sorbitol, unprocessed naproxen, and co-sprayed naproxen and sorbitol from the SASD method (DoE experimental run 12). It can be observed that the unprocessed sorbitol spectra and the SASD-processed powder spectra present a peak at 1053 cm^{-1} and 1047 cm^{-1}, respectively, which corresponds to sorbitol [58]. Sorbitol presents a characteristic absorbance peak at 1046 cm^{-1} associated with C– O stretching vibrations [58,59]. The slight shift in the peak was not attributed to an interaction between naproxen and sorbitol molecules because as concluded in Section 3.2, the interaction between the API and sorbitol is negligible. Additionally, both molecules present a strong and wide peak between 3500 cm^{-1} and 3000 cm^{-1} corresponding to the O-H stretching vibrations [59]. The absence of a peak at/close to 1046 cm^{-1} in the resuspended naproxen particles (after isolation from suspension) indicated the absence of sorbitol. This confirms that sorbitol dissolved upon contact with the aqueous solution releasing the naproxen particles.

5. Conclusions

This work presented a strategy to produce crystalline API particles in an excipient matrix using SASD. The strategy was based on co-spraying a water-soluble excipient namely, sorbitol, with two model APIs, namely indomethacin and naproxen. For naproxen, crystalline particles were obtained, while for indomethacin the particles produced presented a strong amorphous halo in all XRPD patterns. The COSMO-RS modelling conducted revealed that the APIs are not soluble in sorbitol and thus, agreed with the thermal analysis where no interaction between the APIs and excipient was observed. Moreover, COSMO-RS modelling provided insight on how crystallisation occurs in the SASD process, by giving an approximate calculation that in the nozzle all components (e.g. naproxen, indomethacin, sorbitol) should be dissolved in the CO_2/solvent mixture. Regarding the reconstitution of the SASD powdered samples into particle suspensions, for naproxen, using sorbitol during the SASD process generated a powder that could be suspended in an aqueous excipient solution of poloxamer 188 and Tween 20. Naproxen presented the most stable solid form (Form 1) as a dry powder after being isolated from suspension. The particles in suspension had an average size of approximately 2 μm regardless of the experimental conditions used, and a plate-like morphology. The strategy presented could potentially be further developed and implemented to produce resuspendable powders for injection, and could be expanded to more water-soluble excipients and other APIs.

Declaration of Competing Interest

The authors declare the following financial interests/personal relationships which may be considered as potential competing interests. Luis Padrela reports financial support was provided by Enterprise Ireland. Fidel Mendez Canellas reports was provided by EU Framework Programme for Research and Innovation Marie Sklodowska-Curie Actions.

Data Availability

Data will be made available on request.

Acknowledgements

This project has received funding from the European Union's Horizon 2020 Research and Innovation Programme under the Marie Skłodowska-Curie grant agreement (Grant no. 861278). L. Padrela would like to acknowledge Enterprise Ireland for funding support through Grant number CF20170754.

Appendix A. Supporting information

Supplementary data associated with this article can be found in the online version at doi:10.1016/j.supflu.2023.105969.

References

[1] A. Dokoumetzidis, P. Macheras, A century of dissolution research: from Noyes and Whitney to the Biopharmaceutics Classification System, Int. J. Pharm. 321 (2006) 1–11, https://doi.org/10.1016/j.ijpharm.2006.07.011.
[2] K. Sigfridsson, A.J. Lundqvist, M. Strimfors, Particle size reduction and pharmacokinetic evaluation of a poorly soluble acid and a poorly soluble base during early development, Drug Dev. Ind. Pharm. 37 (2011) 243–251, https://doi.org/10.3109/03639045.2010.505927.
[3] A.B. Da Fonseca Antunes, B.G. De Geest, C. Vervaet, J.P. Remon, Solvent-free drug crystal engineering for drug nano- and micro suspensions, Eur. J. Pharm. Sci. 48 (2013) 121–129, https://doi.org/10.1016/j.ejps.2012.10.017.
[4] N. Darville, M. Van Heerden, A. Vynckier, M. De Meulder, P. Sterkens, P. Annaert, G. Van Den Mooter, Intramuscular administration of paliperidone palmitate extended-release injectable microsuspension induces a subclinical inflammatory reaction modulating the pharmacokinetics in rats, J. Pharm. Sci. 103 (2014) 2072–2087, https://doi.org/10.1002/jps.24014.
[5] N.D. Rudd, M. Reibarkh, R. Fang, S. Mittal, P.L. Walsh, A.P.J. Brunskill, W. P. Forrest, Interpreting in vitro release performance from long-acting parenteral nanosuspensions using USP-4 dissolution and spectroscopic techniques, Mol. Pharm. 17 (2020) 1734–1747, https://doi.org/10.1021/acs.molpharmaceut.0c00208.
[6] K. Sigfridsson, A. Lundqvist, M. Strimfors, Subcutaneous administration of nano- and microsuspensions of poorly soluble compounds to rats, Drug Dev. Ind. Pharm. 40 (2014) 511–518, https://doi.org/10.3109/03639045.2013.771645.
[7] C.I. Nkanga, A. Fisch, M. Rad-Malekshahi, M.D. Romic, B. Kittel, T. Ullrich, J. Wang, R.W.M. Krause, S. Adler, T. Lammers, W.E. Hennink, F. Ramazani, Clinically established biodegradable long acting injectables: an industry perspective, Adv. Drug Deliv. Rev. 167 (2020) 19–46, https://doi.org/10.1016/j.addr.2020.11.008.
[8] Y. Shi, A. Lu, X. Wang, Z. Belhadj, J. Wang, Q. Zhang, A review of existing strategies for designing long-acting parenteral formulations: Focus on underlying mechanisms, and future perspectives, Acta Pharm. Sin. B 11 (2021) 2396–2415, https://doi.org/10.1016/j.apsb.2021.05.002.

[9] P. van der Linden, J. Douchamps, C. Schmitt, D. Forget, Ready-to-use injection preparations versus conventional reconstituted admixtures, Pharmacoeconomics 20 (2002) 529–536, https://doi.org/10.2165/00019053-200220080-00003.

[10] Y.H. Jo, W.G. Shin, J.Y. Lee, B.R. Yang, Y.M. Yu, S.H. Jung, H.S. Kim, Evaluation of an intravenous preparation information system for improving the reconstitution and dilution process, Int. J. Med. Inf. 94 (2016) 123–133, https://doi.org/10.1016/j.ijmedinf.2016.07.005.

[11] B.W. Risør, Costs of a Hospital-Based, Ready-To-Use Syringe Delivery Programme Research & Reviews: Journal of Hospital and Clinical Pharmacy Centre for Health Economics Research (COHERE), Department of Public Health, University of Southern Health Outcome Researc, Res. Rev. J. Hosp. Clin. Pharm. (2017).

[12] B. Favier, H. Spath, P. Anhoury, A. Pacull, Pcn29 economic advantages and timesaving of using oxaliplatin concentrated solution versus oxaliplatin lyophilised powder for infusion, Value Heal 9 (2006) A284–A285, https://doi.org/10.1016/s1098-3015(10)63459-6.

[13] C.M. Woon, T.E. Tan, P.Y. Hooi, S.N. Teoh, T.S. Wu, Point-of-care activated system versus conventional intravenous admixture system at an academic medical centre in Singapore, J. Pharm. Pract. Res. 48 (2018) 80–84, https://doi.org/10.1002/jppr.1383.

[14] B. Sinha, R.H. Müller, J.P. Möschwitzer, Bottom-up approaches for preparing drug nanocrystals: Formulations and factors affecting particle size, Int. J. Pharm. 453 (2013) 126–141, https://doi.org/10.1016/j.ijpharm.2013.01.019.

[15] H.K. Chan, P.C.L. Kwok, Production methods for nanodrug particles using the bottom-up approach, Adv. Drug Deliv. Rev. 63 (2011) 406–416, https://doi.org/10.1016/j.addr.2011.03.011.

[16] L. Padrela, M.A. Rodrigues, A. Duarte, A.M.A. Dias, M.E.M. Braga, H.C. de Sousa, Supercritical carbon dioxide-based technologies for the production of drug nanoparticles/nanocrystals – a comprehensive review, Adv. Drug Deliv. Rev. 131 (2018) 22–78, https://doi.org/10.1016/j.addr.2018.07.010.

[17] M. Malamatari, A. Charisi, S. Malamataris, K. Kachrimanis, I. Nikolakakis, Spray drying for the preparation of nanoparticle-based drug formulations as dry powders for inhalation, Processes 8 (2020) 788, https://doi.org/10.3390/pr8070788.

[18] C. Moura, T. Casimiro, E. Costa, A. Aguiar-Ricardo, Optimization of supercritical CO_2-assisted spray drying technology for the production of inhalable composite particles using quality-by-design principles, Powder Technol. 357 (2019) 387–397, https://doi.org/10.1016/j.powtec.2019.08.090.

[19] P. Franco, I.De Marco, Nanoparticles and nanocrystals by supercritical CO_2-assisted techniques for pharmaceutical applications: a review, Appl. Sci. 11 (2021) 1476, https://doi.org/10.3390/app11041476.

[20] V. Verma, P. Patel, K.M. Ryan, S. Hudson, L. Padrela, Production of hydrochlorothiazide nanoparticles with increased permeability using top-spray coating process, J. Supercrit. Fluids 192 (2023), 105788, https://doi.org/10.1016/j.supflu.2022.105788.

[21] B. Long, K.M. Ryan, L. Padrela, From batch to continuous — new opportunities for supercritical CO_2 technology in pharmaceutical manufacturing, Eur. J. Pharm. Sci. 137 (2019), 104971, https://doi.org/10.1016/j.ejps.2019.104971.

[22] B. Long, G.M. Walker, K.M. Ryan, L. Padrela, Controlling polymorphism of carbamazepine nanoparticles in a continuous supercritical-CO_2-assisted spray drying process, Cryst. Growth Des. 19 (2019) 3755–3767, https://doi.org/10.1021/acs.cgd.9b00154.

[23] S. Sala, A. Córdoba, E. Moreno-Calvo, E. Elizondo, M. Muntó, P.E. Rojas, M.À. Larrayoz, N. Ventosa, J. Veciana, Crystallization of microparticulate pure polymorphs of active pharmaceutical ingredients using CO_2-expanded solvents, Cryst. Growth Des. 12 (2012) 1717–1726, https://doi.org/10.1021/cg200356x.

[24] H.T. Wu, C.P. Yang, S.C. Huang, Dissolution enhancement of indomethacin-chitosan hydrochloride composite particles produced using supercritical assisted atomization, J. Taiwan Inst. Chem. Eng. 67 (2016) 98–105, https://doi.org/10.1016/j.jtice.2016.08.012.

[25] L. Padrela, M.A. Rodrigues, S.P. Velaga, A.C. Fernandes, H.A. Matos, E.G. de Azevedo, Screening for pharmaceutical cocrystals using the supercritical fluid enhanced atomization process, J. Supercrit. Fluids 53 (2010) 156–164, https://doi.org/10.1016/j.supflu.2010.01.010.

[26] R. Campardelli, E. Reverchon, Instantaneous coprecipitation of polymer/drug microparticles using the supercritical assisted injection in a liquid antisolvent, J. Supercrit. Fluids 120 (2017) 151–160, https://doi.org/10.1016/j.supflu.2016.11.005.

[27] M.A. Rodrigues, J.M. Tiago, A. Duarte, V. Geraldes, H.A. Matos, Polymorphism in pharmaceutical drugs by supercritical co2 processing: clarifying the role of the antisolvent effect and atomization enhancement, Cryst. Growth Des. 16 (2016) 6222–6229, https://doi.org/10.1021/acs.cgd.6b00697.

[28] J.A. Straub, D.E. Chickering, J.C. Lovely, H. Zhang, B. Shah, W.R. Waud, H. Bernstein, Intravenous hydrophobic drug delivery: a porous particle formulation of paclitaxel (AI-850), Pharm. Res. 22 (2005) 347–355, https://doi.org/10.1007/s11095-004-1871-1.

[29] FDA, INDOCIN (indomethacin) Oral Suspension, for oral use Initial U.S. Approval: 1965, n.d. https://www.accessdata.fda.gov/ (accessed November 13, 2020).

[30] FDA, NAPROSYN (naproxen) Suspension, (n.d.). https://www.accessdata.fda.gov/ (accessed November 13, 2020).

[31] M. Maury, K. Murphy, S. Kumar, A. Mauerer, G. Lee, Spray-drying of proteins: effects of sorbitol and trehalose on aggregation and FT-IR amide I spectrum of an immunoglobulin G, Eur. J. Pharm. Biopharm. 59 (2005) 251–261, https://doi.org/10.1016/j.ejpb.2004.07.010.

[32] G. Elham, P. Mahsa, A. Vatanara, R. Vahid, Spray drying of nanoparticles to form fast dissolving glipizide, Asian J. Pharm. 9 (2015) 213–218, https://doi.org/10.4103/0973-8398.160319.

[33] C.G.C. Paul J. Sheskey, Walter G. Cook, Handbook of pharmaceutical excipients, Eighth edition, Pharm. Press. (2017).

[34] D.M. Aragón, J.E. Rosas, F. Martínez, Solution thermodynamics of naproxen in some volatile organic solvents, Phys. Chem. Liq. 48 (2010) 437–449, https://doi.org/10.1080/00319100902894249.

[35] C.R. Malwade, H. Qu, Cooling crystallization of indomethacin: effect of supersaturation, temperature, and seeding oan polymorphism and crystal size distribution, Org. Process Res. Dev. 22 (2018) 697–706, https://doi.org/10.1021/acs.oprd.8b00078.

[36] W. Zhi, Y. Hu, W. Yang, Y. Kai, Z. Cao, Measurement and correlation of solubility of d-sorbitol in different solvents, J. Mol. Liq. 187 (2013) 201–205, https://doi.org/10.1016/j.molliq.2013.07.014.

[37] J.A. Ferrar, B.D. Sellers, C. Chan, D.H. Leung, Towards an improved understanding of drug excipient interactions to enable rapid optimization of nanosuspension formulations, Int. J. Pharm. 578 (2020), 119094, https://doi.org/10.1016/j.ijpharm.2020.119094.

[38] M. Hugo Silva, S.P. Hudson, L. Tajber, M. Garin, W. Dong, T. Khamiakova, R. Holm, Osmolality of excipients for parenteral formulation measured by freezing point depression and vapor pressure – a comparative analysis, Pharm. Res (2022) 8–11, https://doi.org/10.1007/s11095-022-03262-6.

[39] F. Méndez Cañellas, V. Verma, J. Kujawski, R. Geertman, L. Tajber, L. Padrela, Controlling the polymorphism of indomethacin with poloxamer 407 in a gas antisolvent crystallization process, ACS Omega 7 (2022) 43945–43957, https://doi.org/10.1021/acsomega.2c05259.

[40] N. Hyttinen, N.L. Prisle, Improving solubility and activity estimates of multifunctional atmospheric organics by selecting conformers in COSMO, Therm., J. Phys. Chem. A. 124 (2020) 4801–4812, https://doi.org/10.1021/acs.jpca.0c04285.

[41] BIOVIA COSMOtherm, (2021). ⟨www.3ds.com⟩.

[42] F. Eckert, A. Klamt, Fast solvent screening via quantum chemistry: COSMO-RS approach, AIChE J. 48 (2002) 369–385, https://doi.org/10.1002/aic.690480220.

[43] A. Klamt, V. Jonas, T. Bürger, J.C.W. Lohrenz, Refinement and parametrization of COSMO-RS, J. Phys. Chem. A 102 (1998) 5074–5085, https://doi.org/10.1021/jp980017s.

[44] A. Klamt, Conductor-like screening model for real solvents: a new approach to the quantitative calculation of solvation phenomena, J. Phys. Chem. 99 (1995) 2224–2235, https://doi.org/10.1021/j100007a062.

[45] M. Silva, A. Silva, J. Fernandez-Lodeiro, T. Casimiro, C. Lodeiro, A. Aguiar-Ricardo, Supercritical CO_2-assisted spray drying of strawberry-like gold-coated magnetite nanocomposites in chitosan powders for inhalation, Materials 10 (2017) 74, https://doi.org/10.3390/ma10010074.

[46] R.P. Cabral, A.M.L. Sousa, A.S. Silva, A.I. Paninho, M. Temtem, E. Costa, T. Casimiro, A. Aguiar-Ricardo, Design of experiments approach on the preparation of dry inhaler chitosan composite formulations by supercritical CO_2-assisted spray-drying, J. Supercrit. Fluids 116 (2016) 26–35, https://doi.org/10.1016/j.supflu.2016.04.001.

[47] W. Cho, M.S. Kim, M.S. Jung, J. Park, K.H. Cha, J.S. Kim, H.J. Park, A. Alhalaweh, S.P. Velaga, S.J. Hwang, Design of salmon calcitonin particles for nasal delivery using spray-drying and novel supercritical fluid-assisted spray-drying processes, Int. J. Pharm. 478 (2015) 288–296, https://doi.org/10.1016/j.ijpharm.2014.11.051.

[48] H. Veith, C. Luebbert, G. Sadowski, Correctly measuring and predicting solubilities of solvates, hydrates, and polymorphs, Cryst. Growth Des. 20 (2020) 723–735, https://doi.org/10.1021/acs.cgd.9b01145.

[49] J.S. Song, Y.T. Sohn, Crystal forms of naproxen, Arch. Pharm. Res. 34 (2011) 87–90, https://doi.org/10.1007/s12272-011-0110-7.

[50] A. Nezzal, L. Aerts, M. Verspaille, G. Henderickx, A. Redl, Polymorphism of sorbitol, J. Cryst. Growth 311 (2009) 3863–3870, https://doi.org/10.1016/j.jcrysgro.2009.06.003.

[51] A.E. DeJong, R.W. Hartel, Factors impacting sorbitol polymorphism and polymorphic transitions during aging, J. Food Eng. 253 (2019) 72–78, https://doi.org/10.1016/j.jfoodeng.2019.02.020.

[52] X. Yuan, A.C. Capomacchia, The binary eutectic of NSAIDs and two-phase liquid system for enhanced membrane permeation, Pharm. Dev. Technol. 10 (2005) 1–10, https://doi.org/10.1081/PDT-200035859.

[53] Y. Takebayashi, K. Sue, T. Furuya, S. Yoda, Solubilities of organic semiconductors and nonsteroidal anti-inflammatory drugs in pure and mixed organic solvents: measurement and modeling with hansen solubility parameter, J. Chem. Eng. Data 63 (2018) 3889–3901, https://doi.org/10.1021/acs.jced.8b00536.

[54] S.M. Hitchen, J.R. Dean, Properties of supercritical fluids, in: Appl. Supercrit. Fluids Ind. Anal., Springer, Netherlands, Dordrecht, 1993, pp. 1–11, https://doi.org/10.1007/978-94-011-2146-0_1.

[55] Y. Shimoyama, Y. Iwai, Development of activity coefficient model based on COSMO method for prediction of solubilities of solid solutes in supercritical carbon dioxide, J. Supercrit. Fluids 50 (2009) 210–217, https://doi.org/10.1016/j.supflu.2009.06.004.

[56] A. Tuomela, J. Hirvonen, L. Peltonen, Stabilizing agents for drug nanocrystals: effect on bioavailability, Pharmaceutics 8 (2016) 16, https://doi.org/10.3390/pharmaceutics8020016.

[57] R.C. Rowe, P.J. Sheskey, M.E. Quinn, Handbook of Pharmaceutical Excipients, Pharmaceutical Press, 2009.
[58] E.D.S.G. De Castro, R.J. Cassella, Direct determination of sorbitol and sodium glutamate by attenuated total reflectance Fourier transform infrared spectroscopy (ATR-FTIR) in the thermostabilizer employed in the production of yellow-fever vaccine, Talanta 152 (2016) 33–38, https://doi.org/10.1016/j.talanta.2016.01.054.
[59] S.F. Shaikh, R.S. Mane, B.K. Min, Y.J. Hwang, O. Joo, D-sorbitol-induced phase control of TiO2 nanoparticles and its application for dye-sensitized solar cells, Sci. Rep. 6 (2016) 20103, https://doi.org/10.1038/srep20103.